Elasticity in Thin Films

Mater. Res. Soc. Symp. Proc. Vol. 875 © 2005 Materials Research Society O1.1

Advanced Resonant-Ultrasound Spectroscopy for Studying Anisotropic Elastic Constants of Thin Films

Hirotsugu Ogi, Nobutomo Nakamura, Hiroshi Tanei, and Masahiko Hirao
Graduate School of Engineering Science, Osaka University
Toyonaka, Osaka 560-8531, Japan

ABSTRACT

This paper presents two advanced acoustic methods for the determination of anisotropic elastic constants of deposited thin films. They are resonant-ultrasound spectroscopy with laser-Doppler interferometry (RUS/Laser method) and picosecond-laser ultrasound method. Deposited thin films usually exhibit elastic anisotropy between the film-growth direction and an in-plane direction, and they show five independent elastic constants denoted by C_{11}, C_{33}, C_{44}, C_{66} and C_{13} when the x_3 axis is set along the film-thickness direction. The former method determines four moduli except C_{44}, the out-of-plane shear modulus, through free-vibration resonance frequencies of the film/substrate specimen. This method is applicable to thin films thicker than about 200 nm. The latter determines C_{33}, the out-of-plane modulus, accurately by measuring the round-trip time of the longitudinal wave traveling along the film-thickness direction. This method is applicable to thin films thicker than about 20 nm. Thus, combination of these two methods allows us to discuss the elastic anisotropy of thin films. The results for Co/Pt superlattice thin film and copper thin film are presented.

INTRODUCTION

Elastic constants of thin films are required primarily for three reasons. First, they are indispensable to calculation of internal stresses in a multiphase composite caused by lattice misfit and different thermal-expansion coefficients among constituents. Second, they are needed to calculate elastic strain energy to find a minimum of the free energy for the estimation of possible microstructure. Third, they are capable of evaluating defects because defects such as voids, dislocations, and microcrackings affect the elastic constants through elastic softening. However, measurement of the elastic constants of thin films has never been straightforward due to elastic anisotropy: Thin films, even polycrystalline thin films, show different elastic properties between along the film-growth direction and along an in-plane direction. Such anisotropy originates from texture, columnar structure, oriented microcracks or precipitates, and internal stresses. The thin films then show transverse isotropy or hexagonal symmetry and possess five independent elastic constants C_{ij}:

$$[C_{ij}] = \begin{bmatrix} C_{11} & C_{12} & C_{13} & 0 & 0 & 0 \\ & C_{11} & C_{13} & 0 & 0 & 0 \\ & & C_{33} & 0 & 0 & 0 \\ & & & C_{44} & 0 & 0 \\ & sym. & & & C_{44} & 0 \\ & & & & & C_{66} \end{bmatrix}$$

when the x_3 axis is taken along the film-growth direction, where $C_{66}=(C_{11}-C_{12})/2$. Most existing methods, however, assumed thin films to be isotropic materials and deduced only one or two moduli among five. They failed to detect elastic anisotropy.

The acoustic methods we present in this paper determine four components of C_{ij} among five. They are resonant-ultrasound spectroscopy coupled with laser-Doppler interferometry and picosecond-laser ultrasound method. We demonstrate accuracy and correctness of our methods, showing the results for Co/Pt superlattice thin film and copper thin film.

KEY POINTS FOR AN ACCURATE MEASUREMENT

Previous methods fall in two groups. One is static or quasistatic methods. The other is dynamic methods. Static or quasistatic methods include the microtensile test [1-3], microbending test [4,5], and nanoindentation method. The dynamic methods include the flexural-vibration method [6,7], Brillouin-scattering method [8-10], and surface-acoustic-wave method [11,12]. These previous works involve several difficulties in obtaining the elastic constants of thin films. First of all, static methods are severely affected by errors in dimensions, especially by the film-thickness error. For example, the microbending test evaluates the mechanical behavior of thin films using a cantilever-beam specimen cut from the thin film. The deflection at the free end of the cantilever is proportional to the third power of the film thickness and second power of the width of the cantilever. Thus, the dimension errors have large influence on the measurement. Also, many previous methods are strongly affected by the gripping condition: For example, in the microbending method and flexural-vibration method, the maximum bending stress appears at the fixed end and the measurements are highly affected by the gripping condition because these methods use a simple beam-bending theory, which assumes a complete fixed (rigid) boundary. Besides in the microtensile test, it is difficult to apply a uniaxial stress in the in-plane direction and bending and torsional stresses arise, which affect significantly the stress-strain relationship. In the dynamic methods, such difficulties are less remarkable, but it is still difficult to detect the elastic anisotropy between the in-plane and out-of-plane directions.

We propose three key points for an accurate measurement of the elastic constants. First, measure frequency. Measurement accuracy of resonant frequencies is normally much higher than that for force or displacements. Also, the resonant frequency of a solid is an absolute quantity, which depends only on the mass density, elastic constants, and boundary conditions. Significant advantage of measuring resonant frequencies also involves the fact that they are much less severely affected by dimension errors than static methods, because they are

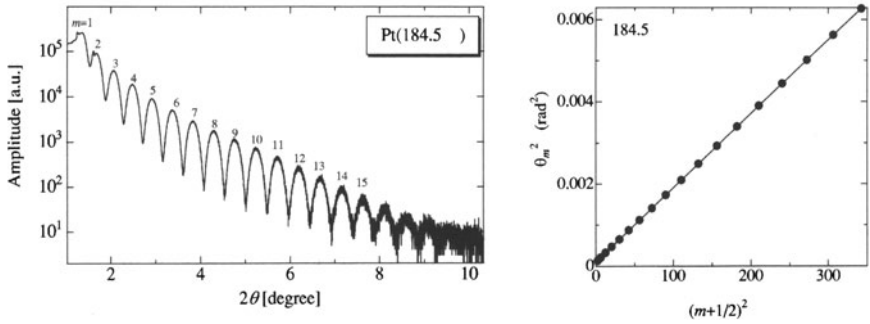

Figure 1. X-ray diffraction spectrum at low angles for platinum thin film with 184.5 Å thickness deposited on a silicon substrate (left), and the correlation between squares of the peak angle and corresponding order number (right). The slope yields the film thickness with known X-ray wavelength.

approximately expressed by $(K/M)^{0.5}$, where K and M denote the stiffness and mass of the system. If we overestimate the film thickness, the mass of the system increases. At the same time, however, the stiffness for bending or torsion increases and the dimension error is canceled.

Second, use free vibrations. Many previous methods involved ambiguous gripping condition at the fixed point. Free-vibration resonant frequencies are hardly affected by gripping conditions and the analysis can be accurate because of free boundaries.

Third, use X rays if possible. Previous works determined the thickness of the film by observing the cross-sectional area of the film with scanning electron microscopy (SEM), which caused 5% error at least. However, when we use an X-ray diffraction measurement, the error can be reduced to less than 1%. For example, Figure 1 shows the X-ray diffraction spectrum in a low-angle region observed from a 185-Å platinum film deposited on a silicon substrate. Many peaks originate from interference between the X ray reflected at the film-substrate interface and that reflected at the film surface. The mth peak angle θ_m is given by [13]

$$\theta_m^2 = \left(\frac{\lambda}{2d}\right)^2 (m+1/2)^2 + \theta_c^2 , \qquad (1)$$

for the platinum-silicon system. Here, d denotes the thickness of the platinum film, λ the X-ray wavelength, and θ_C the critical angle for the total reflection of X ray at platinum surface. Thus, plotting θ_m^2 versus $(m+1/2)^2$ yields a line, whose slope provides the film thickness with known X-ray wavelength (=1.548 Å for Cu-Kα). For a multilayer thin film, the X-ray diffraction spectrum show many peaks related to the bilayer thickness and we can similarly determine the bilayer thickness with the similar way and then the total thickness by multiplying the bilayer thickness by the repetition number [14].

The methodology we present here satisfies these demands. It is a combination of two

advanced methods. They are (i) resonant-ultrasound spectroscopy with laser-Doppler interferometry and (ii) picosecond-laser ultrasound method. The former determines thin-film elastic constants from free-vibration resonant frequencies of the film/substrate specimen via an inverse calculation. This method is sensitive to in-plane moduli such as C_{11} and C_{66}. Its accuracy becomes worse for the out-of-plane moduli C_{33} and C_{13}. It cannot determine the C_{44}, the out-of-plane shear modulus. Thus, this technique determines four independent coefficients among five. We call this method the RUS/Laser technique. The latter method determines C_{33}, the out-of-plane modulus, with accuracy higher than that in any other methods including the RUS/Laser method. It generates the acoustic longitudinal wave propagating along the film-thickness direction by irradiating the film surface with the high-power and short-pulsed laser beam (pumping light). The pulse-echo signals of the longitudinal wave are detected by the delayed pulse light (probing light) through photoelastic phenomena.

Thus, combination of these methods allows us to determine the four moduli and to discuss the elastic anisotropy.

RUS/LASER METHOD

Resonant-ultrasound-spectroscopy (RUS) method has been applied to many anisotropic solids including monocrystals [15,16], composites [17,18], and piezoelectric materials [19-22]. It is capable of determining all the independent elastic constants from resonance frequencies; because all the elastic constants contribute to free-vibration resonant frequencies, they can be determined inversely by measuring the resonant frequencies with sufficient accuracy. This method, however, has not been successfully applied to thin films because of three difficulties. First, the resonant frequencies have to be measured with high accuracy because contributions of the elastic constants of the thin film to them are small; normalized contribution is about in the order of 10^{-2} for a 1-μm-thick film deposited on a 0.2-mm-thick substrate. Second, external forces applied to the specimen have to be eliminated to cause ideal free vibrations. Third, observed modes must be identified. At the beginning of the inverse calculation, we have to homologize individual measured frequency to calculated one. Because we exactly know vibration modes of calculated frequencies, we have to identify the observed frequencies.

The RUS/laser method overcomes these difficulties. We developed a piezoelectric tripod illustrated in Fig. 2. The tripod consists of the needle piezoelectric oscillator, needle piezoelectric detector, and a needle support. The specimen is placed on the tripod without using any coupling media between them. We apply a sinusoidal signal to the piezoelectric transducer to vibrate the specimen. The piezoelectric receiver detects the vibration of the specimen. By sweeping the frequency of the driving signal and acquiring the vibration amplitude as a function of the frequency, we obtain the resonance spectrum as shown in Fig. 3. The resonance frequencies are determined by the Lorentzian-function fitting. This setup requires no external force applied to the specimen except the specimen's weight, which allows us to carry out generating ideal free vibrations. The piezoelectric tripod we developed works for a very light-weight specimen with the mass about a few milligrams. Measurements were performed in a vacuum, eliminating damping and acoustic noise and at a constant temperature, eliminating its influence on the elastic properties of the films.

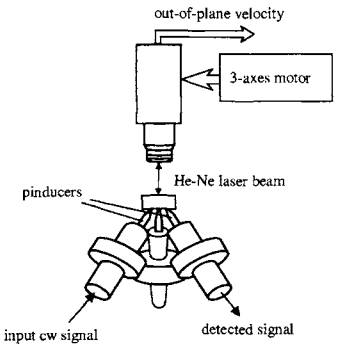

Figure 2. Measurement setup of the RUS/Laser method.

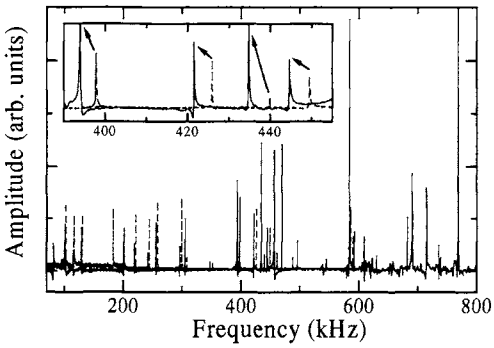

Figure 3. Resonance spectra measured by the piezoelectric tripod. Broken line shows the spectrum for a monocrystal silicon with dimensions of 6x4x0.2 mm^3 and solid line shows that after the 0.89-nm Co/Pt superlattice film was deposited on the substrate.

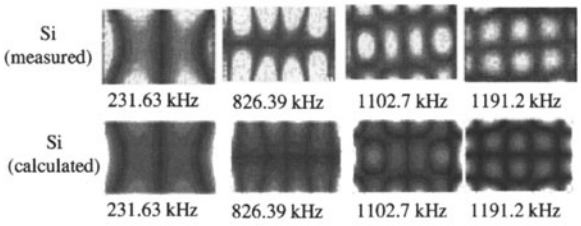

Figure 4. Measured and calculated amplitude distributions of the out-of-plane displacement for a monocrystal silicon of of 6x4x0.2 mm^3.

The weak and stable acoustic coupling provides high accuracy and high reproducibility in the resonance-frequency measurement. Once a specimen is placed on the tripod, the fluctuation of measured frequencies are smaller than one part of million. The accuracy is still high among completely independent measurements, better than one part of 10,000.

Concerning mode identification, we measure distributions of the out-of-plane displacement amplitude on the vibrating specimen using laser-Doppler interferometry. They are then compared with the distributions calculated by the Rayleigh-Ritz method as shown later. Figure 4 shows examples of such comparison: Excellent agreement is always confirmed so that we identify all the observed vibration modes.

Actual procedure to determine the elastic constants are following: (i) The resonant frequencies of a silicon substrate are measured and their modes are identified. (ii) A thin film is deposited on it and resonant frequencies are measured again to record the changes of the

resonant frequencies by identifying the vibration mode to find correct mode correspondence. (iii) Because the changes of the resonant frequencies can be calculated with sufficient accuracy as shown later, the elastic constants of the deposited thin film are determined by a least-squares-fitting procedure.

Analytic solutions of displacements and resonant frequencies at free vibrations are unavailable for the film/substrate specimen of rectangular-parallelepiped shape. However, they are approximately calculated by Lagrangian minimization with Rayleigh-Ritz method, which successfully satisfies accuracy required to determine reliable thin-film elastic constants through the inverse calculation [14,23]. Lagrangian for a solid subjected to free vibration is given by

$$L = \frac{1}{2}\int_V \left(S_i C_{ij} S_j - \rho\omega^2 u_i u_i\right) dV \,. \tag{2}$$

Where S_i is the engineering strain, C_{ij} the elastic constants, ρ the mass density, ω the angular resonant frequency of the system, u_i the displacement along the x_i axis, and V the volume of the film/substrate system. We make approximate estimates for displacements by linear combinations of basis functions Ψ_k

$$u_i(x_1, x_2, x_3) = \sum_k a_k^i \Psi_k^i(x_1, x_2, x_3) \,. \tag{3}$$

Here a_k denote the expansion coefficients and they provide us with the displacement distributions as show in Fig. 4. For a film/substrate rectangular parallelepiped, strains associated with the film-thickness direction (along the x_3 axis) are discontinuous across the interface because of the different moduli. Thus, we have to select basis functions that can express the broken gradients of the displacements across the interface. For this, Heyliger [24] showed that incorporation of one-dimensional Lagrangian interpolation polynomials along the x_3 direction gave good approximates for the displacements in a layered material. Thus, we use the basis functions which consist of one-dimensional Lagrangian interpolation polynomials for the x_3 direction $\xi(x_3)$ and power series for the in-plane directions (x_1 and x_2 axes):

$$\psi_k(x_1, x_2, x_3) = \left(\frac{x_1}{L_1}\right)^l \left(\frac{x_2}{L_2}\right)^m \xi_n(x_3) \,. \tag{4}$$

Here, L_1 and L_2 denote the length of the specimen along the x_1 and x_2 axes, respectively. l, m, and n are integer expressing the orders of the basis functions. Seeking the minimum of the Lagrangian, the problem is reduced to an eigenvalue problem:

$$\omega^2[\mathbf{M}]\{\mathbf{U}\} = [\mathbf{K}]\{\mathbf{U}\}. \tag{5}$$

Here, [**M**] and [**K**] are matrices related to the kinetic energy and strain energy of the system, respectively. {**U**} is the eigenvector composed of the expansion coefficients a_k and it provides

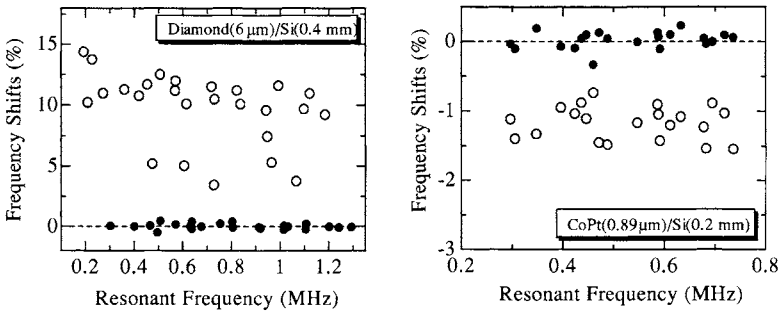

Figure 5. Changes of resonant frequencies by deposition of thin films (open marks) and differences between calculated and measured resonant frequencies (solid marks) for 6-μm-CVD-diamond film on 0.4-mm silicon substrate (left) and 0.89-μm-Co/Pt-superlattice film on 0.2-mm silicon substrate (right).

the displacement distributions through Eq. (3).

Inclusion of higher-order basis functions leads to more accurate resonance frequencies, but it takes longer calculation time. We found that use of the in-plane functions satisfying $l+m<17$ and the out-of-plane functions with $n<11$ lead to resonant frequencies with high enough accuracy and a suitable calculation time [14]. (In this case, the matrix size reaches 5000x5000, but the calculation time is drastically reduced when we consider the symmetry of vibration [14].)

Figure 5 shows resonant-frequency shifts caused by deposition of chemical-vapor-deposition (CVD) diamond film and Co/Pt superlattice film on silicon substrates. Deposition of the CVD diamond increases the resonant frequencies by 5-15% and deposition of Co/Pt superlattice film decreases them by 1-1.5 %. Resonant frequencies of the film/substrate systems are successfully calculated by the inverse calculation with the Lagrangian minimization, indicating reliable elastic constants of the thin films are determined. The rms difference between the measured and calculated resonant frequencies is typically less than 0.1%.

Figure 6 shows contributions of the thin-film elastic constants to the resonant frequencies. The RUS/Laser method is sensitive to in-plane moduli such as C_{11}, C_{12}, and C_{66} because most observed vibration modes are bending and torsional vibrations, causing larger in-plane deformation. However, it is insensitive to out-of-plane moduli such as C_{13}, C_{33}, and C_{44} because of smaller strains along the out-of-plane direction. Especially, C_{44}, the out-of-plane shear modulus, little affects the resonant frequencies and it is unavailable.

Figure 7 demonstrates tolerance of the RUS/Laser method to the error involved in film thickness. These results are for 1-μm and 3-μm copper thin films deposited on the 0.2-mm monocrystal silicon substrate. We artificially included the film-thickness error Δd in the inverse calculation. The resultant errors in the elastic constants are proportional to the film-thickness error. When the film thickness is measured by the cross-sectional observation by SEM with a 5% error, less than 5% errors are caused in the principal elastic constants.

Thus, the RUS/Laser method is capable of determining in-plane elastic constants with high

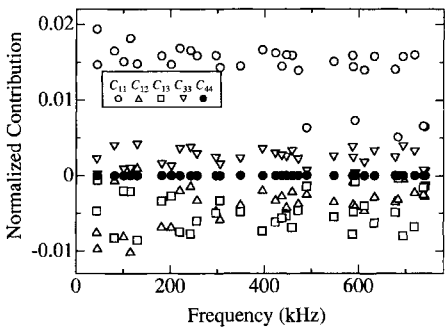

Figure 6. Contributions of the thin-film C_{ij} to resonant frequencies for 0.9-μm CoPt/0.2-mm Si system. C_{44} (solid circles) little contributes to frequencies.

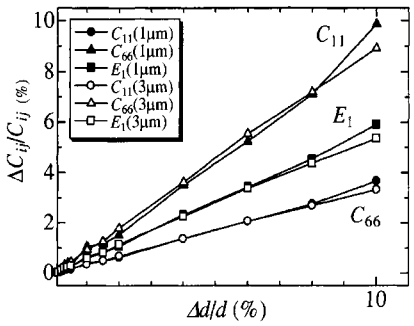

Figure 7. Errors in the principal elastic constants caused by the film-thickness measurement error in the case of copper thin films deposited on 0.2-mm-thick silicon substrate.

accuracy and it is less severely affected by dimension errors. This method is applicable to thin films as thin as 200 nm, although the accuracy gets worse as the thickness decreases.

PICOSECOND-LASER ULTRASOUND METHOD

The picosecond-laser ultrasound method determines C_{33}, the out-of-plane modulus, of films thicker than 20 nm using pulse echoes of the longitudinal wave traveling along the film-thickness direction generated by the thermoelastic or photoelastic effect. There are several pioneers of this method [25-27] and following them we developed the measurement system shown in Fig. 8.

We use a mode-locking titanium-sapphire pulse laser with 100-fs pulse width and 0.7-W power. The laser beam is split into two beams by a polarization beam splitter. One of the beams enters the second-harmonic-generator crystal, which outputs the light with the doubled frequency (pumping light). It is modulated by an acousto-optic modulator and then is focused on the surface of the film through the objective lens to generate the longitudinal wave. The longitudinal wave propagates along the film-thickness direction and repeats reflections between the film/substrate interface and the film surface. The other light is split into two beams; one enters the photo detector to produce the reference signal and the other irradiates the specimen surface with a time delay compared with the arrival time of the pumping light. By changing the path length of the pumping light, we can change the time delay between the pumping and probing lights and we can detect the arrival of the longitudinal wave by monitoring the modified intensity and phase of the reflected probing light. Figure 9 shows an example of such a measurement for 77-nm Co/Pt thin film. Step at t=29 ps indicates the time when the pumping beam irradiated the film surface. Clearly, pulse echoes of the longitudinal wave are observed, which yield the round-trip time and then the C_{33}.